

Supplementary Information

**One-step synthesis of red/green dual-emission carbon dots  
for ratiometric sensitive ONOO<sup>-</sup> probing and cell imaging**

Juanjuan Liu<sup>1,2</sup>, Yanyan Dong<sup>1,2</sup>, Yunxia Ma<sup>1,2</sup>, Yangxia Han<sup>1,2</sup>, Sudai Ma<sup>1,2</sup>, Hongli  
Chen<sup>1,2</sup>, and Xingguo Chen\*<sup>1,2,3</sup>

<sup>1</sup> State Key Laboratory of Applied Organic Chemistry, Lanzhou University, Lanzhou  
730000, China

<sup>2</sup> Department of Chemistry, Lanzhou University, Lanzhou 730000, China

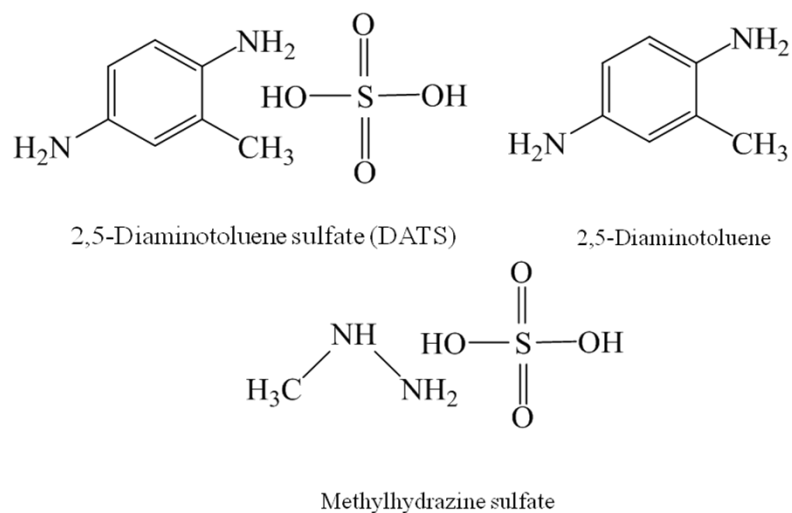
<sup>3</sup> Key Laboratory of Nonferrous Metal Chemistry and Resources Utilization of Gansu  
Province, Lanzhou University, Lanzhou 730000, China

\* Corresponding author

E-mail address: chenxg@lzu.edu.cn

Tel: 86-931-8912763

Fax: 86-931-8912582



**Scheme S1.** Structural formulas of 2,5-diaminotoluene sulfate, 2,5-diaminotoluene and methylhydrazine sulfate.

**Table S1.** Comparison of the properties of the RGDE CDs with other CDs.

Synthetic raw material	Single/dual emission	Excitation wavelength (nm)	Emission wavelength (nm)	QY (%)	Reference
citric acid, urea, sodium fluoride	single	530	600	1.20	1
citric acid, neutral red	single	530	632	12.1	2
p-phenylenediamine	single	470	620	15.0	3
ascorbic acid, ethylene glycol	dual	365	435/538	not mentioned	4
m-phenylenediamine, sulfuric acid	dual	300	360/520	43.0 (460 nm excitation)	5
citric acid, urea	dual	380	455/520	14.0 (420 nm excitation)	6, 7
2,5-diaminotoluene sulfate	dual	380	525/603	9.00 (380 nm excitation)	this work

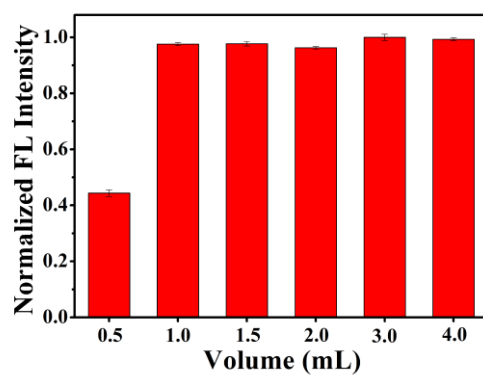


**Fig. S1.** Effect of ethanol volume on the fluorescence intensity (603 nm) of the RGDE CDs.

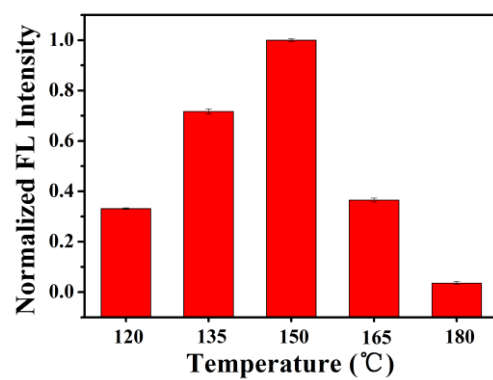


**Fig. S2.** Effect of reaction temperature on the fluorescence intensity (603 nm) of the RGDE CDs.

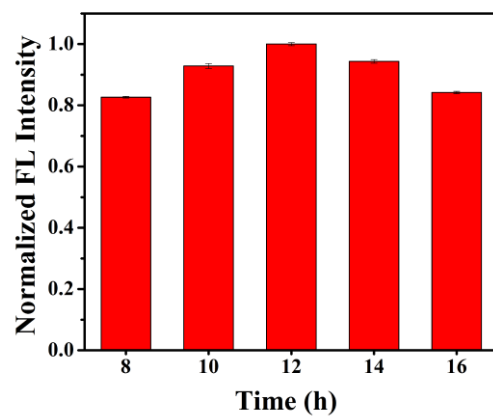


**Fig. S3.** Effect of reaction time on the fluorescence intensity (603 nm) of the RGDE CDs.

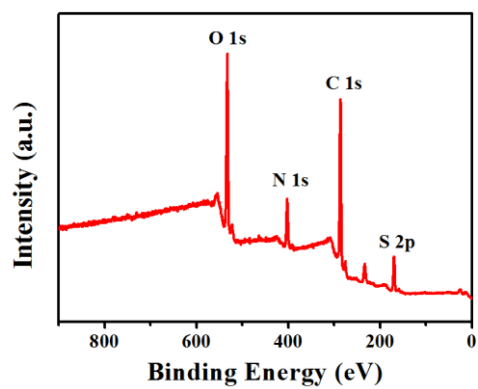


**Fig. S4.** XPS full-scan spectrum of the RGDE CDs.

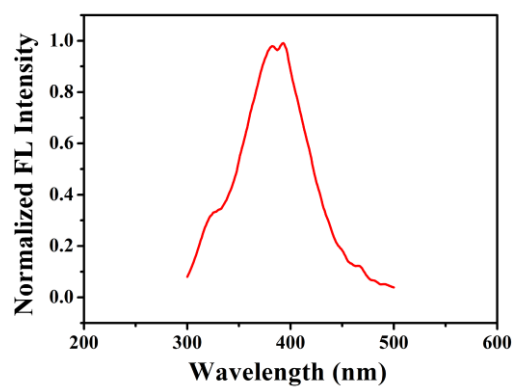


**Fig. S5.** Fluorescence excitation spectrum of the RGDE CDs.



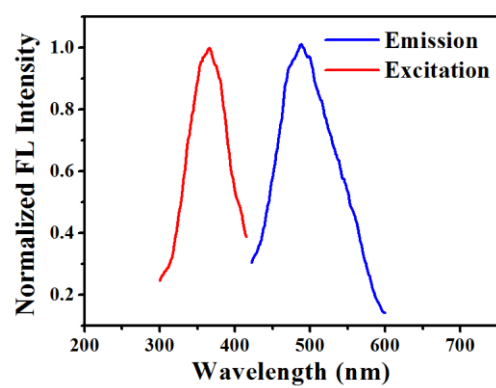


**Fig. S6.** Fluorescence excitation and emission spectra of the CDs prepared through using 2,5-diaminotoluene as carbon source.

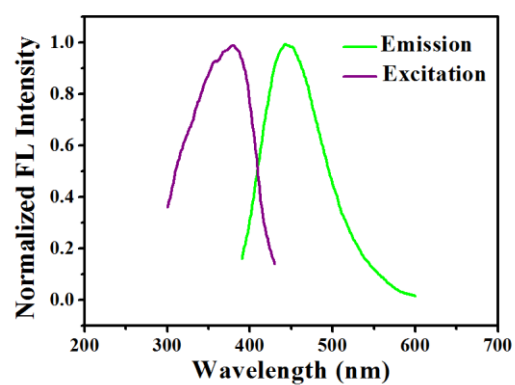


**Fig. S7.** Fluorescence excitation and emission spectra of the CDs prepared through using methylhydrazine sulfate as carbon source.

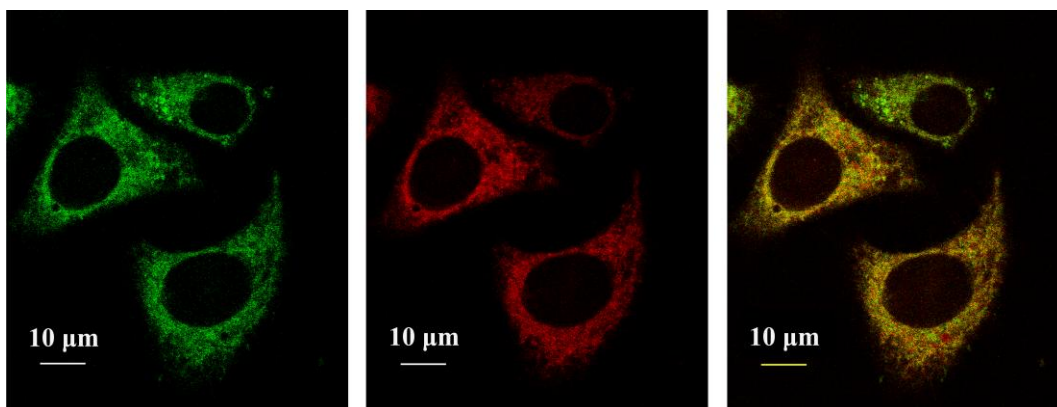


**Fig. S8.** Confocal microscopy fluorescence images of HeLa cells treated with the RGDE CDs (30  $\mu\text{g}/\text{mL}$ ) in green channel, red channel and merged image of green and red channel. Scale bar is 10  $\mu\text{m}$ .

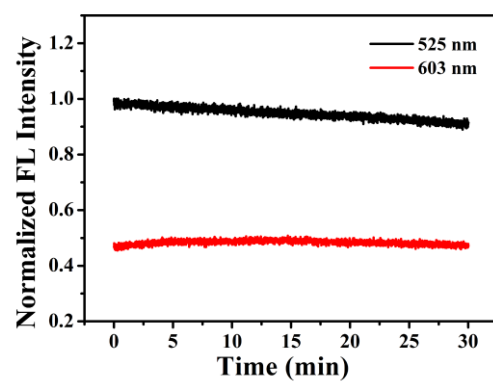


**Fig. S9.** Effect of light illumination time on the fluorescence intensity of the RGDE CDs.

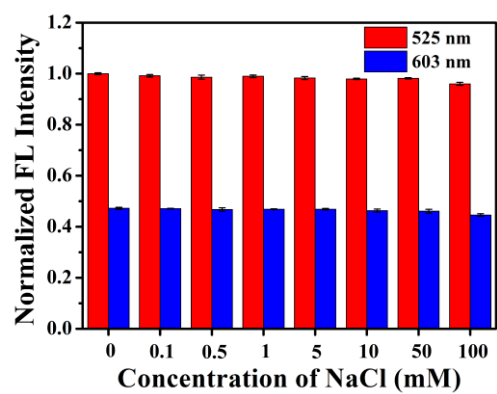


**Fig. S10.** Effect of concentration of NaCl solution on the fluorescence intensity of the RGDE CDs.

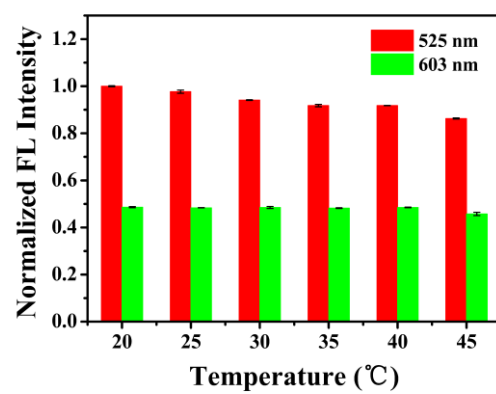


**Fig. S11.** Effect of environmental temperature on the fluorescence intensity of the RGDE CDs.

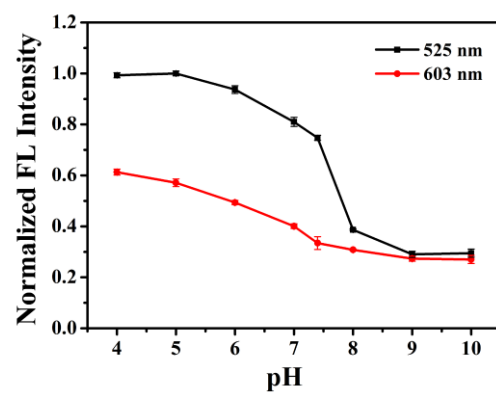


**Fig. S12.** Effect of pH of buffer solution on the fluorescence intensity of the RGDE CDs.

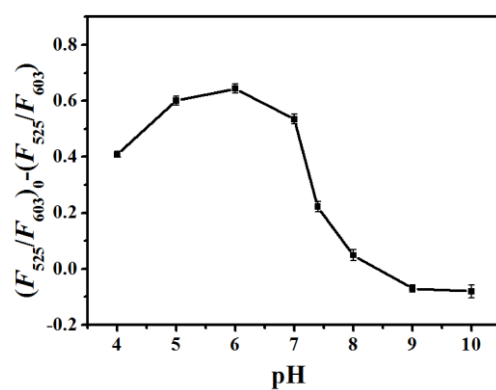


**Fig. S13.** Effect of pH of buffer solution on  $(F_{525}/F_{603})_0$  and  $(F_{525}/F_{603})$ .  $(F_{525}/F_{603})_0$  and  $(F_{525}/F_{603})$  were the fluorescence intensity ratios of the RGDE CDs solution in the absence and presence of  $22 \mu\text{M ONOO}^-$ , respectively.



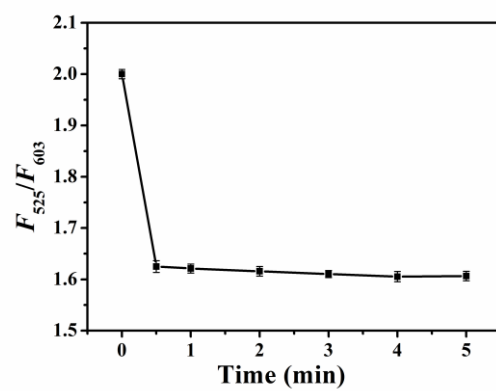


**Fig. S14.** Time-dependent fluorescence intensity of the RGDE CDs with the addition of 22  $\mu\text{M}$   $\text{ONOO}^-$  at room temperature.

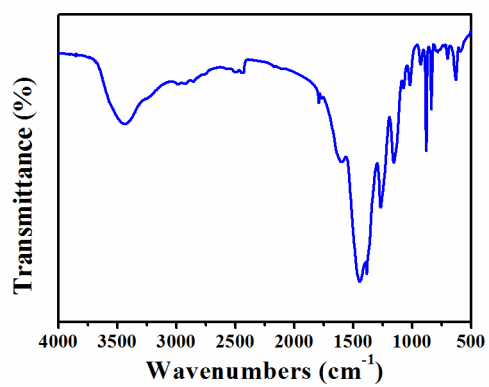


**Fig. S15.** FT-IR spectrum of the RGDE CDs in the presence of  $\text{ONOO}^-$ .

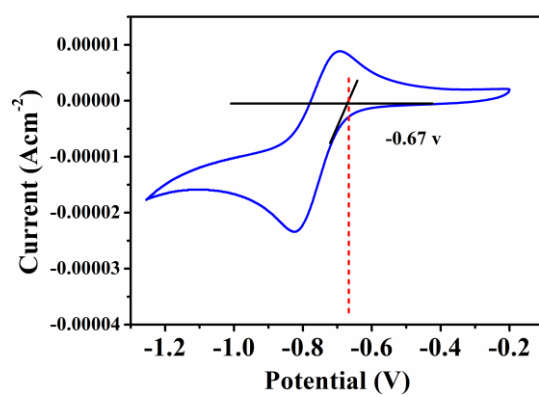


**Fig. S16.** Cyclic voltammograms of the RGDE CDs in the solution state (solvent: freshly dried dimethylformamide).

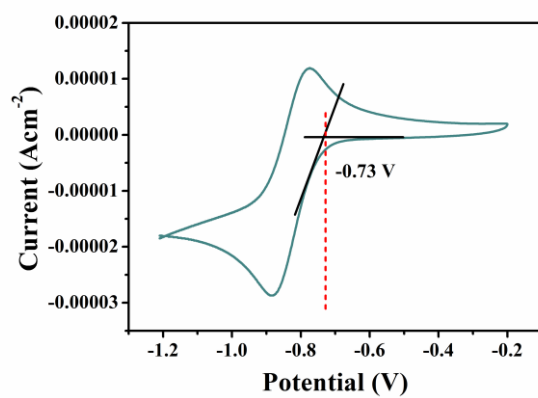


**Fig. S17.** Cyclic voltammograms of  $\text{ONOO}^-$  in the solution state (solvent: freshly dried dimethylformamide).

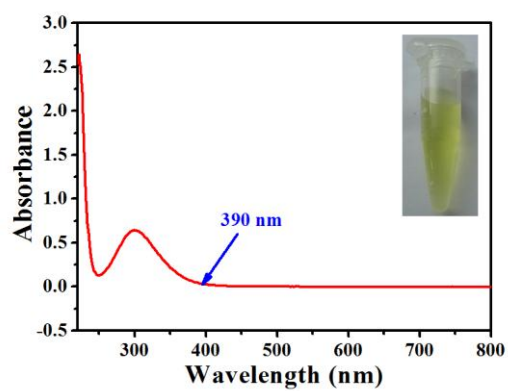


**Fig. S18.** UV-vis absorption spectrum of  $\text{ONOO}^-$ , inset was the photograph of  $\text{ONOO}^-$  solution under visible light.

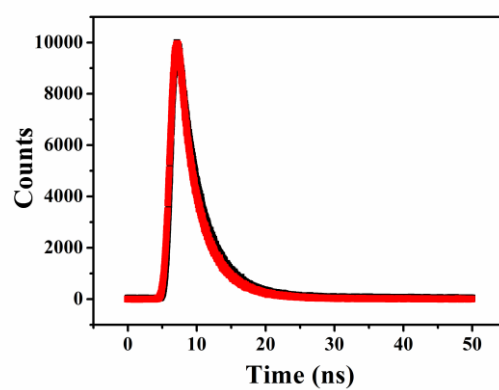


**Fig. S19.** Time-resolved decays of the RGDE CDs in the absence (black line) and presence (red line) of  $\text{ONOO}^-$ .

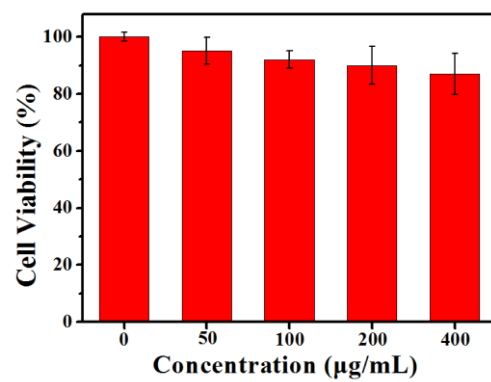


**Fig. S20.** Cell viability of HeLa cells with different concentrations of the RGDE CDs.

### Quantum yield (QY) measurements.

QY of the obtained RGDE CDs was determined by the method mentioned in our previous work.<sup>8</sup> The absolute photoluminescence quantum yield can be represented simple in the equation below:

$$QY = \frac{\int L_{\text{emission}}}{\int E_{\text{solvent}} - \int E_{\text{sample}}} \quad (1)$$

where QY was the absolute quantum yield,  $L_{\text{emission}}$  was the fluorescence (FL) emission spectrum of the RGDE CDs sample, collected using the sphere;  $E_{\text{sample}}$  was the spectrum of the light used to excite the sample, collected using the sphere;  $E_{\text{solvent}}$  was the spectrum of the light used for excitation with only the solvent in the sphere, collected using the sphere. The solvent in this experiment was deionized water.



## References

1. W. Yang, H. Zhang, J. Lai, X. Peng, Y. Hu, W. Gu and L. Ye, *Carbon*, 2018, **128**, 78-85.
2. W. Gao, H. Song, X. Wang, X. Liu, X. Pang, Y. Zhou, B. Gao and X. Peng, *ACS Appl. Mater. Interfaces*, 2018, **10**, 1147-1154.
3. Y. Sun, X. Wang, C. Wang, D. Tong, Q. Wu, K. Jiang, Y. Jiang, C. Wang and M. Yang, *Microchim. Acta*, 2018, **185**, 83.
4. R. Mohan, J. Drbohlavova and J. Hubalek, *Chem. Phys. Lett.*, 2018, **692**, 196-201.
5. W. Zhou, J. Zhuang, W. Li, C. Hu, B. Lei and Y. Liu, *J. Mater. Chem. C*, 2017, **5**, 8014-8021.
6. S. Qu, X. Wang, Q. Lu, L. X. Liu and L. Wang, *Angew. Chem.*, 2012, **124**, 12381-12384.
7. S. Qu, H. Chen, X. Zheng, J. Cao and X. Liu, *Nanoscale*, 2013, **5**, 5514-5518.
8. J. Feng, Y. Chen, Y. Han, J. Liu, C. Ren and X. Chen, *Anal. Chim. Acta*, 2016, **926**, 107-117.